

Increased Myocardial Uptake of Dietary Fatty Acids Linked to Cardiac Dysfunction in Glucose-Intolerant Humans

Sébastien M. Labbé,¹ Thomas Grenier-Larouche,¹ Christophe Noll,¹ Serge Phoenix,^{1,2} Brigitte Guérin,² Eric E. Turcotte,² and André C. Carpentier¹

Impaired cardiac systolic and diastolic function has been observed in preclinical models and in subjects with type 2 diabetes. Using a recently validated positron emission tomography (PET) imaging method with 14(*R,S*)-[¹⁸F]-fluoro-6-thia-heptadecanoic acid to quantify organ-specific dietary fatty acid partitioning, we demonstrate in this study that overweight and obese subjects with impaired glucose tolerance (IGT⁺) display significant increase in fractional myocardial dietary fatty acid uptake over the first 6 h postprandial compared with control individuals (IGT⁻). Measured by [¹¹C]acetate with PET, IGT⁺ subjects have a significant increase in myocardial oxidative index. IGT⁺ subjects have significantly reduced left ventricular stroke volume and ejection fraction (LVEF) and tend to display impaired diastolic function, as assessed by PET ventriculography. We demonstrate an inverse relationship between increased myocardial dietary fatty acid partitioning and LVEF. Fractional dietary fatty acid uptake is reduced in subcutaneous abdominal and visceral adipose tissues in IGT⁺ directly associated with central obesity. Fractional dietary fatty acid uptake in skeletal muscles or liver is, however, similar in IGT⁺ versus IGT⁻. The current study demonstrates, for the first time, that excessive myocardial partitioning of dietary fatty acids occurs in prediabetic individuals and is associated with early impairment of left ventricular function and increased myocardial oxidative metabolism. *Diabetes* 61:2701–2710, 2012

Elevation of circulating fatty acids in humans has been shown to induce insulin resistance and impair β -cell function (1). Prediabetic and diabetic subjects display inefficient adipose tissue storage of dietary fatty acids during the postprandial state (2). This may lead to increased postprandial triglyceride (TG) and/or nonesterified fatty acid (NEFA) circulating levels produced from dietary fatty acids with increased flux of dietary fatty acids to lean tissues (3,4) that is directly related to the presence of abdominal obesity (5). Despite this elevated NEFA flux in type 2 diabetes (T2D), muscle NEFA uptake is not necessarily elevated because of reduced postprandial muscle blood flow (6). Regulation

of tissue dietary fatty acid uptake is complex and involves lipoprotein lipase (LpL)-mediated TG lipolysis, and cellular membrane transporter-mediated NEFA uptake that may be differentially activated in the various tissues (7). Thus, the contribution of dietary fatty acids to organ-specific postprandial fatty acid exposure cannot be assessed simply by measurement of circulating NEFA and TG fluxes.

Increased cardiac LpL-mediated uptake of fatty acids in mice leads to lipotoxicity and impaired cardiac function (8). We have recently developed a noninvasive method using the oral administration of 14(*R,S*)-[¹⁸F]-fluoro-6-thia-heptadecanoic acid (¹⁸FTHA), a long-chain fatty acid analog, measured with positron emission tomography (PET) to assess organ-specific partitioning of dietary fatty acids in rodents and humans (9). We showed in diabetic rats an increase in myocardial dietary fatty acid uptake associated with maintained cardiac oxidative metabolism in the face of reduced contractile function (10).

We aimed to determine whether organ-specific dietary fatty acid partitioning, cardiac function, and myocardial energy metabolism are abnormal in obese, impaired glucose-tolerant (IGT⁺) individuals. We hypothesized that IGT⁺ subjects would display an increase in myocardial dietary fatty acid partitioning associated with reduced left ventricular function and reduced adipose tissue storage of dietary fatty acids.

RESEARCH DESIGN AND METHODS

Study participants. Seventeen healthy Caucasian subjects without (IGT⁻: 11 men and 6 women) and nine subjects with glucose intolerance defined as having a 2-h post-75-g oral glucose tolerance test between 7.8 and 11.1 mmol/L on two occasions (IGT⁺: four men and five women), aged between 18 and 60 years, underwent two postprandial metabolic studies. Subjects with history or clinical evidence of any cardiac disorder, any evidence for kidney, liver, or thyroid dysfunction, or any uncontrolled medical or surgical condition were excluded. Subjects taking any antidiabetic medication (except metformin), β -blocker, fibrates, or with a history of any dietary or severe past allergic reaction or who participated in any research trial involving radiation exposure within the past 12 months were also excluded. Those subjects who had dyslipidemia and were on a statin (one control and four IGT participants) or had hypertension and were treated with antihypertensive agents (two IGT participants) had to stop these medications 3 weeks and 7 days, respectively, prior to the metabolic assessments. One participant who was on metformin discontinued the medication (with approval of her attending physician) several weeks prior to the study.

Experimental protocols. The subjects followed an isocaloric diet (0% alcohol, 15% protein, 30% fat, and 55% carbohydrates) 48 h before each experimental protocol. On arrival, body weight, height and waist circumference were measured, and lean body mass was determined by electrical bioimpedance (Hydra ECF/ICF; Xitron Technologies, San Diego, CA). An intravenous catheter was placed in one forearm for infusions, and another was placed in the contralateral arm maintained in a heating pad (~55°C) for blood sampling.

Each participant underwent two 6-h postprandial experimental protocols (A and B), performed within 4 weeks of each other in random order, in which a standard liquid meal prepared as described (5) was consumed by the participants (400 mL over 20 min for a total of 906 kcal, 33 g or 33% as fat, 34 g or

From the ¹Department of Medicine, Division of Endocrinology, Centre de Recherche Clinique Etienne-LeBel, Université de Sherbrooke, Sherbrooke, Québec, Canada; and the ²Department of Nuclear Medicine and Radiobiology, Centre de Recherche Clinique Etienne-LeBel, Université de Sherbrooke, Sherbrooke, Québec, Canada.

Corresponding author: André C. Carpentier, andre.carpentier@usherbrooke.ca. Received 22 December 2011 and accepted 24 April 2012.

DOI: 10.2337/db11-1805

This article contains Supplementary Data online at <http://diabetes.diabetesjournals.org/lookup/suppl/doi:10.2337/db11-1805/-/DC1>.

© 2012 by the American Diabetes Association. Readers may use this article as long as the work is properly cited, the use is educational and not for profit, and the work is not altered. See <http://creativecommons.org/licenses/by-nc-nd/3.0/> for details.

See accompanying commentary, p. 2659.

17% as proteins, and 101 g or 50% as carbohydrates). Blood samples were collected in tubes containing Na₂EDTA and Orlistat (30 µg/mL; Roche, Mississauga, Ontario, Canada) to prevent in vitro TG lipolysis.

In protocol A, we used our novel oral ¹⁸FTHA method (9) to determine whole-body dietary fatty acid partitioning. ¹⁸FTHA given orally is absorbed through chylomicron-TG, delivered into the circulation from the thoracic duct, and redistributes normally into other circulating fatty acid pools (9). This method assumes ¹⁸FTHA-containing chylomicron-TG hydrolysis and uptake in local tissue microcirculation that are similar to that of chylomicron-TG not containing ¹⁸FTHA. Each subject was positioned supine and scanned using a 16-slice PET/computed tomography (CT) scanner (Philips Gemini TF; Philips, Eindhoven, NV) (9). At time 0 min, ~70 MBq ¹⁸FTHA produced as previously described (11) was mixed into Intralipid 20% (Baxter, Mississauga, Ontario, Canada), incorporated into gel capsules (T.U.B Enterprises) and given orally with the liquid meal. After a segmental CT (40 mAs) to measure hepatic radiodensity and for definition of PET regions of interest (ROI), dynamic list-mode PET scanning centered on the thoracoabdominal segment was performed between time 90 and 120 min (15 × 120 s) after meal intake to determine oral ¹⁸FTHA uptake rate in the heart and liver. At time 360 min, whole-body PET/CT acquisition was performed to determine ¹⁸FTHA tissue distribution and uptake (9). The maximal gastrointestinal tract radioactivity exposure for oral ¹⁸FTHA administration was estimated at 2.35 mSv at the stomach. One of the IGT⁻ participants suffered a migraine by the end of this protocol, and whole-body PET/CT scanning at time 360 min was therefore not performed.

In protocol B, 90 min after the start of meal intake, [¹¹C]acetate (~185MBq) was administered intravenously over 30 s with dynamic list-mode PET acquisition for 30 min (18 × 10 s, 6 × 30 s, and 6 × 240 s) centered on the thoracoabdominal segment to determine cardiac perfusion and oxidative metabolic index using multicompartamental modeling (6,12). Electrocardiogram (ECG) gating was performed in all but our first four consecutive participants, allowing the application of PET ventriculography to determine cardiac function (10).

Total radioactivity exposure to the participants was <18 mSv including the two protocols. All tracers were tested for sterility and nonpyrogenicity.

PET/CT image analyses. For dynamic PET acquisitions, mean value of pixels (mean kbq/mL) for each frame was recorded. ROI were drawn on the heart (three consecutive 5-mm slices starting from the middle of the long cardiac axis toward the cardiac valves), liver, and thoracic aorta to generate tissues and blood time-radioactivity curves. The ROI were first defined from the transaxial CT slices and then copied to ¹⁸FTHA and [¹¹C]acetate image sequences. Myocardial and hepatic fractional dietary fatty acid uptakes (*K_i*) were determined using Patlak linearization (10). Input function was taken from the aorta, and we showed that no correction is needed for spillover and partial volume effect in this instance because the diameter of the aorta is large enough (13). For these analyses, it was assumed that all circulating dietary fatty acids and ¹⁸FTHA were circulating in chylomicron-TG between times 90 and 120 min (9). Myocardial and liver dietary fatty acid uptake (*K_m*) was then calculated by multiplying *K_i* by chylomicron-TG levels. For whole-body scans, mean value of pixels (mean standard uptake value [SUV]) for all tissues of interest were recorded. ROI were drawn on the liver, heart, quadriceps femoris, thigh, and anterior abdominal subcutaneous adipose tissues, and right perirenal adipose tissue (a visceral adipose tissue depot; this depot was chosen to avoid gastric and intestinal spillover of ¹⁸F activity that occurred in most other splanchnic adipose tissue depots) (9).

Cardiac blood flow index [*K₁* in min⁻¹ of [¹¹C]acetate, with correction for first-pass tissue extraction (14)] and oxidative metabolism index (*K₂* in min⁻¹ of [¹¹C]acetate) were estimated from [¹¹C]acetate using a three-compartment model (12) as previously published (6). For analysis of ventricular function, PET data from [¹¹C]acetate images were obtained as a series of 16 per heartbeat ECG-gated frames and reconstructed as a series of adjacent two-dimensional slices using 20 iterations of the maximum-likelihood expectation maximization algorithm. The Corridor4DM v5.2 clinical software (Segami; Invia) was used for reorientation and to compute left ventricular volumes, left ventricular ejection fraction, stroke volume, cardiac output, left ventricular peak filling rate, left ventricular early mean filling rate, and time-to-peak filling rate. In two of the IGT⁻ participants, only eight per heartbeat ECG-gated frames could be reconstructed such that left ventricular diastolic function indexes are unavailable for these two participants.

Laboratory assays and assessment of insulin resistance. Glucose, insulin, total NEFA, and TG were measured as described (5). Chylomicrons and plasma lipids were separated by ultracentrifugation and assayed for ¹⁸F activity and TG concentration (9). The homeostasis model assessment insulin resistance index (HOMA-IR) was calculated (as in Ref. 15): glucose (in mmol/L) · insulin (in mU/L)/22.5.

Statistical analyses. Data are expressed as mean ± SEM. Mann-Whitney, two-way ANOVA for repeated measures, or χ² tests were used when appropriate.

Spearman correlations were performed to examine association between variables. A two-tailed *P* value <0.05 was considered significant. All comparisons between IGT⁺ and IGT⁻ groups were prespecified, but other analyses were post hoc and should be viewed as hypothesis generating. All analyses were performed with the JMP software for Windows, version 7.0 (SAS Institute, Cary, NC), or GraphPad Prism version 5.00 for Windows (GraphPad, San Diego, CA).

Study approval. Informed written consent was obtained in accordance with the Declaration of Helsinki, and the protocol received approval from the Human Ethics Committee of the Centre de Recherche Clinique Etienne-LeBel.

RESULTS

Anthropometric characteristics, postprandial plasma metabolites, and insulin levels and circulating ¹⁸FTHA metabolites. As shown in Table 1, IGT⁺ participants were older, more insulin resistant, and had higher BMI, waist circumference, and nonlean mass but a similar lean mass. Plasma glucose (Fig. 1A) was higher in IGT⁺ throughout the metabolic study (two-way ANOVA, *P* < 0.001). Plasma insulin, NEFA, and TG levels (respectively; Fig. 1B–D) were all significantly higher in IGT⁺ participants (two-way ANOVA, *P* < 0.001). Chylomicron-TG levels were, however, lower in IGT⁺ (two-way ANOVA, *P* < 0.001) (Fig. 1E).

As shown in Fig. 2A, we determined that dietary fatty acids reached the circulation at similar rate in both groups. Moreover, we measured the ¹⁸F activity in chylomicrons (Fig. 2B), total TG (Fig. 2C), and NEFA (Fig. 2D). IGT⁻ and IGT⁺ subjects showed similar rate of chylomicrons excursion in plasma and the same rate of spillover lipolysis (¹⁸F-NEFA) into the circulation.

TABLE 1
Characteristics of the participants

	IGT ⁻ (n = 17)	IGT ⁺ (n = 9)	<i>P</i> value
Age (years)	45 (3)	54 (3)	0.04
Sex (male:female)	11:6	4:5	0.09
Weight (kg)	85.1 (4.6)	90.8 (4.4)	0.32
BMI (kg/m ²)	28.3 (1.0)	31.4 (0.95)	0.05
Waist (cm)	90 (4)	103 (3)	0.02
Lean mass (kg)	57.2 (3.3)	52.1 (4.0)	0.31
Nonlean mass (kg)	27.9 (2.6)	38.8 (3.9)	0.04
HOMA-IR	2.28 (0.28)	5.39 (0.51)	0.0002
Fasting glucose (mmol/L)	4.5 (0.1)	5.3 (0.2)	0.003
Fasting insulin (pmol/L)	81 (9)	166 (15)	0.0004
Fasting NEFA (µmol/L)	357 (34)	511 (57)	0.03
Fasting TG (mmol/L)	1.4 (0.3)	1.8 (0.2)	0.09
Statin use (n)	1	4	0.001
Statin dose (% maximum)	50	62.5 (21.7)	—
ARB use (n)	—	1	—
ARB dose (% maximum)	—	10	—
ACEI use (n)	—	1	—
ACEI dose (% maximum)	—	80	—

Data are mean (SEM) unless otherwise indicated. *P* values are from Mann-Whitney tests for continuous variables and from χ² test for frequency data. Note that medications were stopped prior to metabolic testing of the participants. ACEI, angiotensin-converting enzyme inhibitors; ARB, angiotensin II receptor blockers.

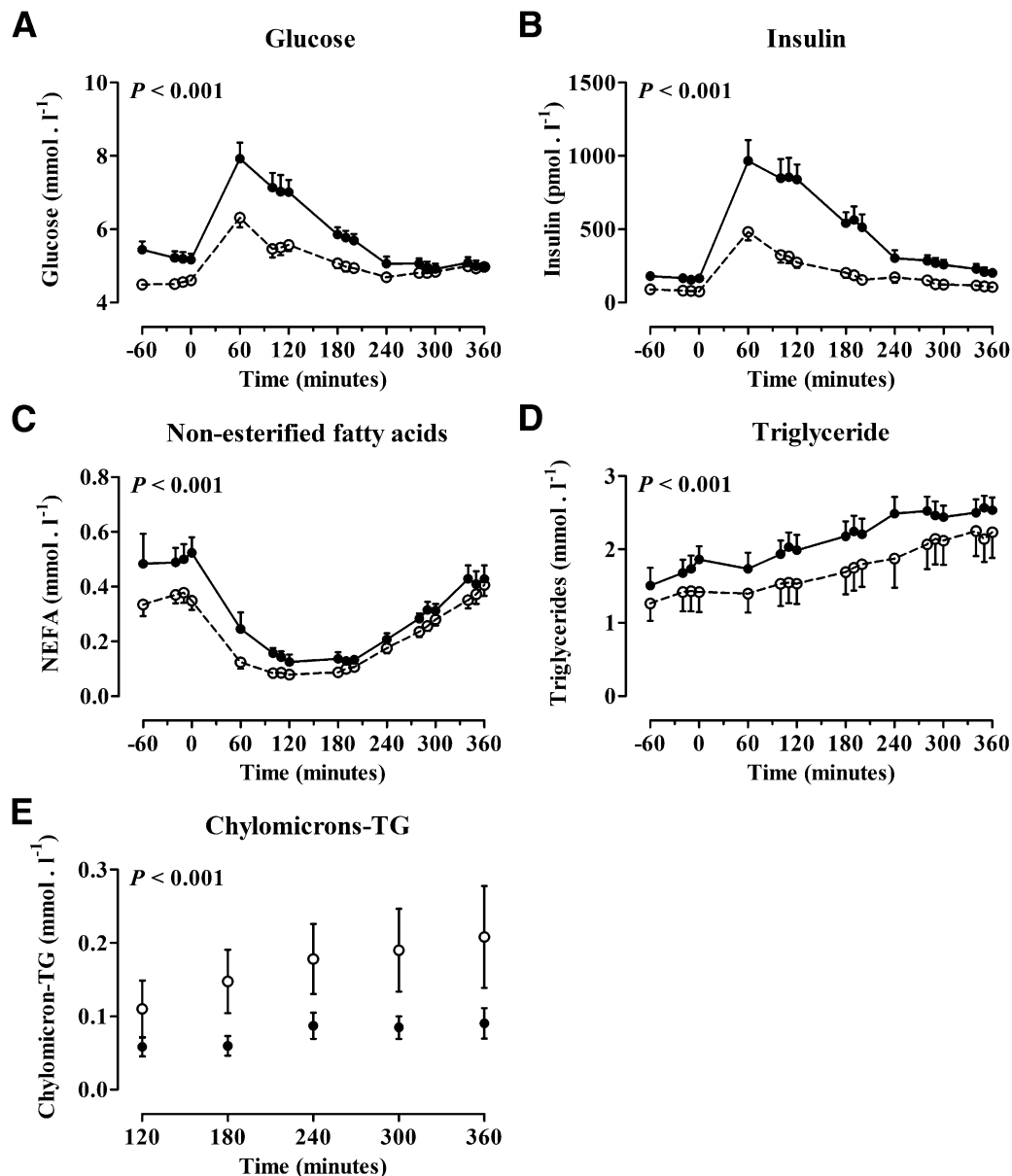


FIG. 1. Plasma glucose (A), insulin (B), NEFA (C), TG (D), and chylomicron-TG (E) excursion after standard liquid meal intake at time 0. *P* values are two-way ANOVA comparisons between groups in a model that also included time and time \times group interaction. ●, IGT⁺; ○, IGT⁻.

Organ-specific partitioning of dietary fatty acids and cardiac and hepatic fractional and net uptake rates. Whole-body PET acquisition showing relative biodistribution of orally administered ¹⁸FTHA 6 h after meal ingestion is shown in one of the IGT⁻ (Fig. 3A) and one of the IGT⁺ (Fig. 3B) subjects. Relative myocardial dietary fatty acid uptake (Fig. 3C) was increased by 63% in IGT⁺ subjects (2.13 ± 0.21 vs. 1.31 ± 0.17 SUV units; $P = 0.01$). There were no significant changes in dietary fatty acid biodistribution (IGT⁺ vs. IGT⁻) in the liver (Fig. 3D: 3.57 ± 0.47 vs. 3.35 ± 0.47 SUV units; $P = 0.55$), skeletal muscles (Fig. 3E: 0.27 ± 0.05 vs. 0.22 ± 0.04 SUV units; $P = 0.48$), and thigh subcutaneous adipose tissue (Fig. 3F: 0.07 ± 0.02 vs. 0.08 ± 0.02 SUV units; $P = 0.75$). We noted, however, a 54 and 58% reduction, respectively, in relative tracer uptake in anterior abdominal subcutaneous (0.11 ± 0.02 vs. 0.24 ± 0.03 SUV units; $P = 0.02$) and perirenal (0.17 ± 0.03 vs. 0.41 ± 0.06 SUV units; $P = 0.006$) adipose tissue depots (Fig. 3G and H) in

IGT⁺ vs. IGT⁻ subjects. Radiodensity of the liver was similar in IGT⁻ and IGT⁺ subjects (52.5 ± 1.8 vs. 45.1 ± 3.8 Hounsfield units; $P = 0.17$).

Early myocardial dietary fatty acid fractional uptake (Fig. 4A) was increased (0.066 ± 0.013 vs. 0.022 ± 0.005 min⁻¹; $P = 0.003$) in IGT⁺ subjects from dynamic acquisitions between times 90 and 120 min after meal ingestion. Myocardial net uptake from chylomicrons was not significantly higher in IGT⁺ (Fig. 4B: 3.60 ± 0.99 vs. 1.77 ± 0.57 nmol \cdot g⁻¹ \cdot min⁻¹; $P = 0.15$) during this phase. Early liver fractional (Fig. 4C: 0.077 ± 0.027 vs. 0.050 ± 0.012 min⁻¹; $P = 0.42$) and net (Fig. 4D: 6.04 ± 3.24 vs. 6.07 ± 2.45 nmol \cdot g⁻¹ \cdot min⁻¹; $P = 0.97$) uptake of dietary fatty acids from chylomicrons was similar in both groups.

Left ventricular function and myocardial blood flow and oxidative metabolism indexes. Table 2 shows blood pressure, heart rate, left ventricular volumes and function, and myocardial blood flow and oxidative metabolic indexes

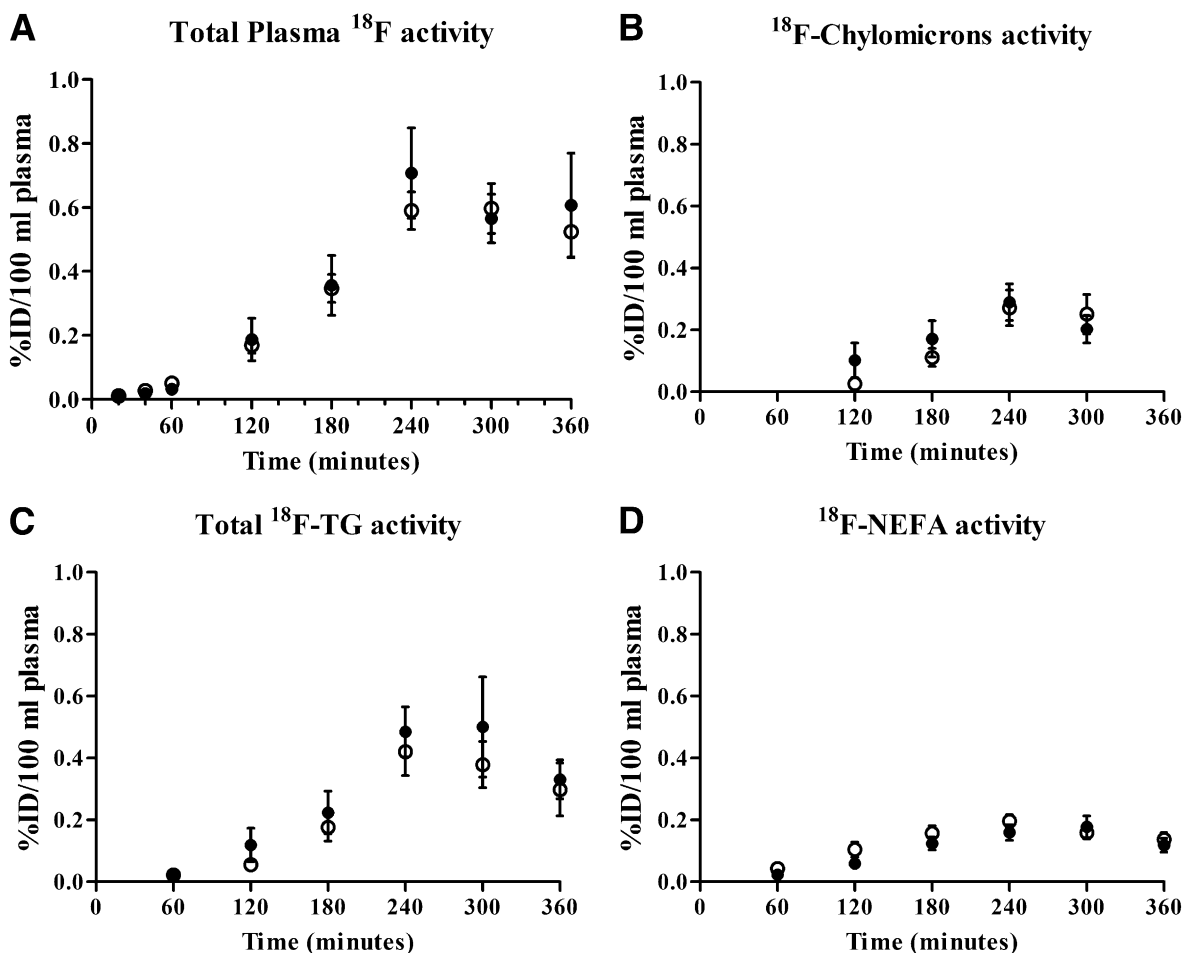


FIG. 2. ^{18}F activity in plasma (A), chylomicron fraction (B), plasma TG (C), and plasma NEFA (D) after oral administration of 14(*R,S*)- ^{18}F THA. Data were analyzed using two-way ANOVA with group, time, and time \times group interaction as independent variables in the model. None of the group comparisons were significant. ID, ingested dose. ●, IGT+; ○, IGT-.

from [^{11}C]acetate PET dynamic and ECG-gated postprandial acquisitions. Blood pressure, heart rate, and the rate-pressure product were similar in both groups. The left ventricular stroke volume, fractional ejection fraction, and cardiac output were significantly reduced in IGT $^{+}$ subjects. Early left ventricular peak filling rate was lower and time-to-peak filling rate was longer in IGT $^{+}$ subjects. IGT $^{+}$ participants also had higher myocardial blood flow and oxidative indexes.

Correlates of myocardial and adipose tissue relative dietary fatty acid uptake. Relative myocardial dietary fatty acid uptake was associated with lower systolic blood pressure (Table 3), lower left ventricular fraction (Fig. 5A), lower left ventricular stroke volume (Fig. 5B), higher time-to-peak filling rate of the left ventricle (Fig. 5C), and higher myocardial oxidative index (Fig. 5D). Relative myocardial dietary fatty acid uptake was, however, not significantly associated with age, sex, HOMA-IR, BMI, or waist circumference (Table 3). Relative hepatic and skeletal muscle dietary fatty acid uptake were not associated with age, anthropometric characteristics, or cardiac function (Table 3). Relative visceral adipose tissue dietary fatty acid uptake was associated with younger age (Table 3), lower fasting glucose, insulin, NEFA, and TG levels, lower HOMA-IR, and lower waist circumference (Fig. 5E), whereas relative anterior subcutaneous abdominal adipose tissue

dietary fatty acid uptake was associated with younger age, lower glucose, insulin, and TG levels, lower HOMA-IR, lower BMI, lower waist circumference (Fig. 5F), higher liver radiodensity (e.g., inversely related to liver fat content), higher left ventricular ejection fraction, and higher ventricular peak filling rate (Table 3). Relative subcutaneous thigh adipose tissue dietary fatty acid uptake was associated with lower TG levels, lower BMI, lower waist circumference, lower systolic blood pressure, and lower cardiac rate-pressure product (Table 3).

Cardiac fractional dietary fatty acid uptake determined by Patlak analysis was also significantly associated with higher insulin levels, higher HOMA-IR, lower left ventricular stroke volume and early mean filling rate, lower cardiac output, higher time-to-peak left ventricular filling rate, and higher myocardial oxidative index (Supplementary Table 1). Liver fractional dietary fatty acid uptake was higher in women and significantly associated with lower TG levels and higher myocardial oxidative index (Supplementary Table 1).

DISCUSSION

Novel findings of the current study include: 1) significant increase in fractional myocardial dietary fatty acid uptake in IGT $^{+}$ individuals not explained by difference in age,

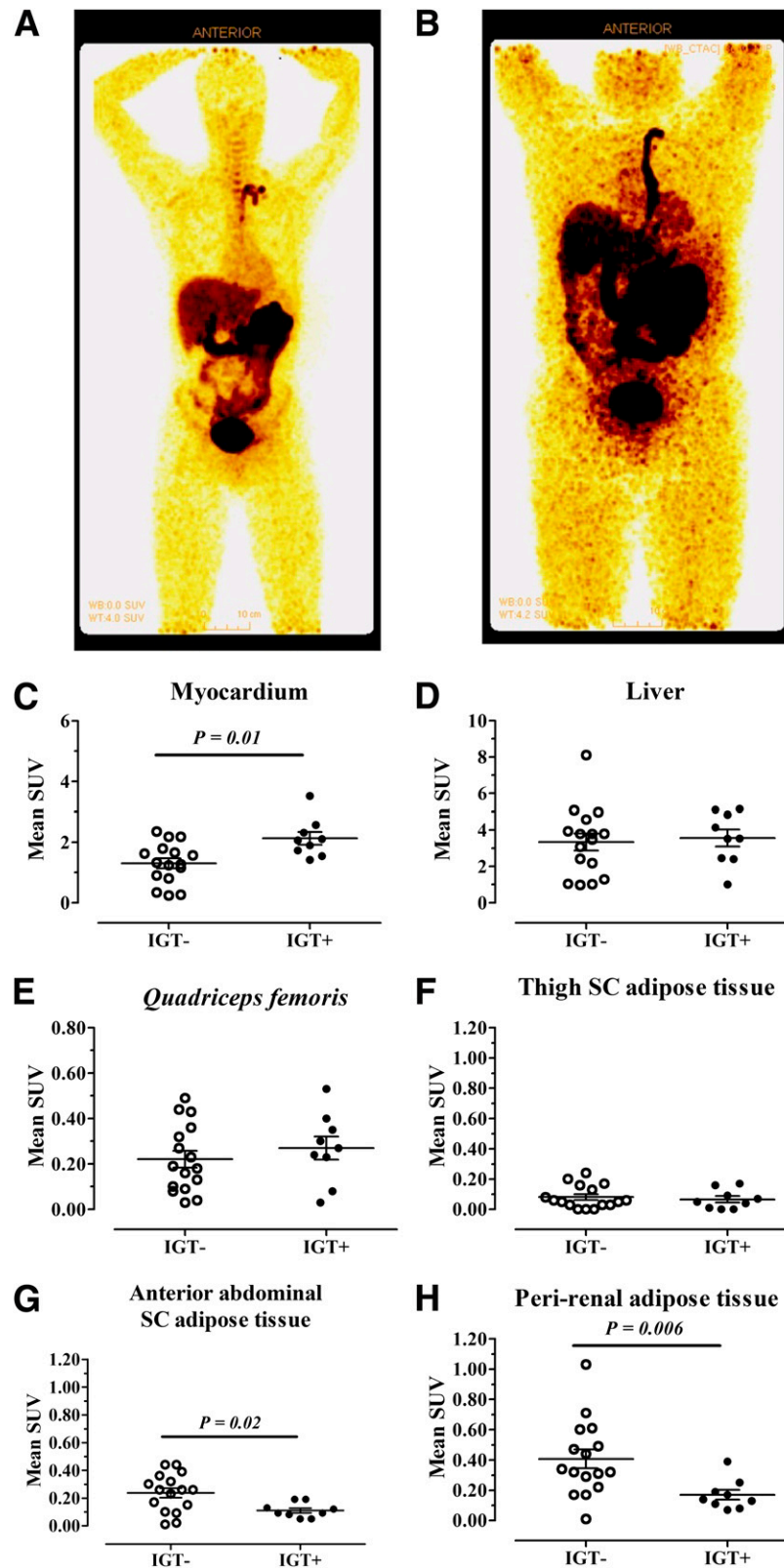


FIG. 3. Anteroposterior whole-body PET acquisition performed 6 h after oral administration of $14(R,S)$ - ^{18}F THA from an IGT⁻ (A) and IGT⁺ subject (B). SUV from whole-body PET in the heart (C), liver (D), skeletal muscle (E), thigh subcutaneous (SC) adipose tissue (F), anterior SC abdominal adipose tissue (G), and perirenal adipose tissue (H). P values are from Mann-Whitney test. (A high-quality digital representation of this figure is available in the online issue.)

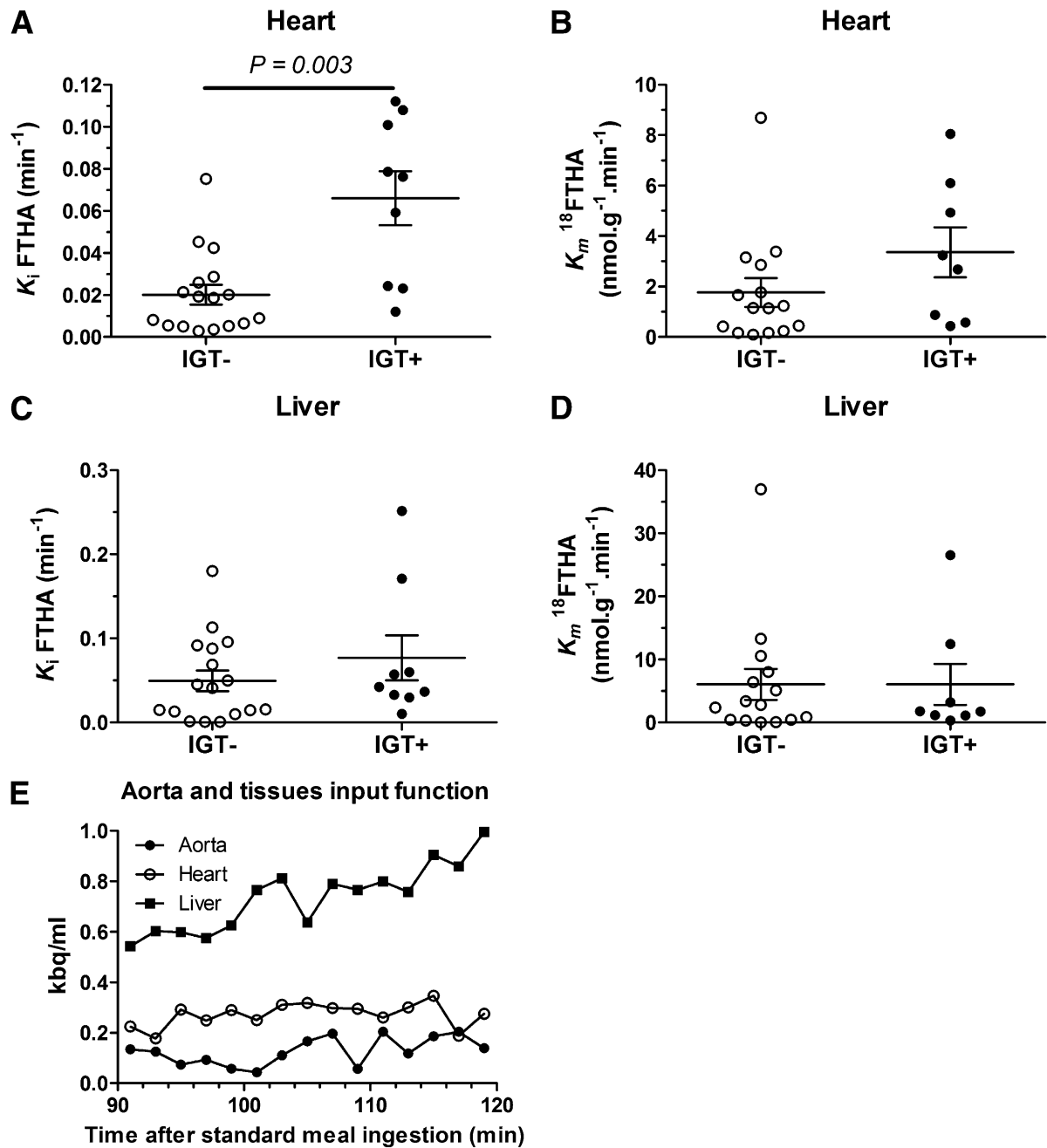


FIG. 4. Fractional $14(R,S)$ - ^{18}F THA uptake rate in the heart (A) and liver (C) and net chylomicron-fatty acid uptake rate in the heart (B) and liver (D) between times 90 and 120 min after oral administration of the tracer. Radioactivity in aorta (closed circles), left ventricle (open circles), and liver (closed squares) during dynamic PET acquisition is shown from a representative participant (E). P values are from Mann-Whitney test.

body fat, central obesity markers, or sex; 2) an association between the latter myocardial metabolic abnormality and reduction in systolic and diastolic left ventricular functions and increased myocardial oxidative metabolism; and 3) no significant changes in liver and skeletal muscle dietary fatty acid uptake in IGT+ individuals. The present results extend the association between increased myocardial NEFA uptake and oxidation and IGT observed during fasting (16) to postprandial dietary fatty acids. In addition, we confirmed the findings of others of reduced subcutaneous abdominal and visceral adipose tissue fractional uptake of dietary fatty acids in abdominally obese individuals (17,18). We furthermore found a direct association

between impaired relative dietary fatty acid uptake in abdominal subcutaneous adipose tissue and lower left ventricular ejection fraction and increased liver steatosis.

Increased oxidative metabolism in the face of similar or reduced mechanical work is the hallmark of diabetic cardiomyopathy (19) and obesity (16). In humans, some degree of cardiac systolic and diastolic dysfunction has been observed very early after onset of T2D (20–22). Fatty acids impair myocardial insulin signaling, and lipotoxicity has been implicated in the cardiomyopathy associated with T2D in rodents (19,23). The presence of a small absolute increase in intramyocardial TG content has been demonstrated by proton magnetic resonance spectroscopy in prediabetic and

TABLE 2
Left ventricular volumes, function, blood flow index, and oxidative metabolism index

	IGT ⁻	IGT ⁺	<i>P</i> value
End-systolic volume (mL)*	36 (3)	42 (6)	0.42
End-diastolic volume (mL)*	113 (7)	104 (9)	0.38
Stroke volume (mL)*	77 (4)	62 (4)	0.04
Left ventricular ejection fraction (%)*	69 (1)	61 (2)	0.002
Heart rate (min ⁻¹)	68 (2)	72 (2)	0.39
Cardiac output (mL/min)*	5272 (236)	4305 (250)	0.03
Left ventricular peak filling rate†**	3.03 (0.16)	2.78 (0.20)	0.58
Left ventricular early mean filling rate†**	1.88 (0.05)	1.61 (0.13)	0.08
Time-to-peak filling rate (ms)**	122 (8)	144 (12)	0.11
Systolic blood pressure (mmHg)	125 (2)	128 (4)	0.79
Diastolic blood pressure (mmHg)	74 (2)	76 (2)	0.77
Rate-pressure product (mmHg · min ⁻¹)	8541 (328)	9141 (569)	0.52
Blood flow index (min ⁻¹)	1.224 (0.104)	1.832 (0.233)	0.04
Oxidative metabolism index, <i>k</i> ₂ (min ⁻¹)	0.032 (0.009)	0.130 (0.027)	0.001

Data are mean (SEM) unless otherwise indicated. *P* values are from Mann-Whitney test. *In *n* = 15 IGT⁻ and 7 IGT⁺ participants. †Units are fractional end diastolic volume per second. **In *n* = 13 IGT⁻ and 7 IGT⁺ participants.

diabetic humans (24,25). Although myocardial TG deposition occurs at increased rate during fasting compared with the postprandial period in healthy subjects (26), cardiac non-oxidative fatty acid metabolism is a small fraction of total

myocardial fatty acid uptake (11,16), potentially explaining discordant findings between proton-magnetic resonance spectroscopy and our present method. Increased reliance on fatty acid oxidation may lead to reduced myocardial energy efficiency and predispose to increased damage if ischemia is superimposed (25,27). Excess intake of dietary fatty acids may contribute to the development and progression of heart failure (28,29). Recently, we showed increased myocardial dietary fatty acid uptake in high-fat/high-fructose-fed plus streptozotocin-injected rats (10). We previously demonstrated that acute elevation of circulating TG using intravenous intralipid infusion leads to reduced myocardial glucose uptake in rats (30). Reduced myocardial glucose utilization appears to be an early feature of high fat-induced insulin resistance and cardiac dysfunction in mice (31). Cardiac transgenic expression of LpL also leads to lipotoxic cardiomyopathy (8), demonstrating that increased myocardial uptake of fatty acids from circulating TG is a candidate mechanism for cardiac dysfunction in hypertriglyceridemic states, including prediabetes and T2D.

We found higher meal fatty acid storage per volume of tissue in subcutaneous abdominal than in subcutaneous leg adipose tissue, a finding consistent with most (17,32–35) but not all (36) previous studies. We found a trend toward higher dietary fatty acid uptake per volume of tissue in lower body subcutaneous adipose tissues in women versus men, a finding also observed in some previous studies (34,36), but not in others (32,33). In the few studies that measured fatty acid uptake in visceral adipose depots using biopsies, relative uptake tended to be higher in the former than in subcutaneous adipose tissues (17,37,38), also consistent with the observations of the current study. In accordance with our findings, all previous studies comparing lean versus obese individuals found that the latter display significantly lower dietary fatty acid uptake per mass of adipose tissue (17,18).

TABLE 3
Correlates of organ-specific relative dietary fatty acid uptake

	Heart	Liver	Visceral adipose tissue	SC abdominal adipose tissue	Skeletal muscle	SC thigh adipose tissue
IGT (IGT ⁺ = 1)	0.51**	0.13	-0.57**	-0.48*	0.15	-0.07
Age	0.14	-0.06	-0.42*	-0.45*	-0.18	-0.30
Sex (male = 0; female = 1)	0.13	0.29	-0.05	0.22	0.36	0.37
BMI	0.03	-0.17	-0.39	-0.58**	-0.11	-0.47*
Waist circumference	0.10	-0.12	-0.51**	-0.68***	-0.11	-0.42*
HOMA-IR	0.24	-0.09	-0.47*	-0.47*	-0.03	-0.31
Fasting glucose	0.01	-0.02	-0.48*	-0.50**	0.16	-0.03
Fasting insulin	0.25	-0.08	-0.42*	-0.45*	-0.02	-0.29
Fasting NEFA	0.16	-0.02	-0.41*	-0.30	-0.01	-0.09
Fasting TG	-0.20	-0.40*	-0.52**	-0.78***	-0.30	-0.44*
Liver radiodensity	0.06	0.16	0.29	0.57***	0.01	0.23
Stroke volume	-0.45*	-0.22	0.39	-0.09	-0.10	-0.13
Left ventricular ejection fraction	-0.45*	-0.08	0.33	0.47*	-0.07	0.09
Heart rate	0.07	-0.14	-0.37	-0.19	-0.16	-0.25
Systolic blood pressure	-0.41*	-0.15	-0.31	-0.32	-0.30	-0.44*
Diastolic blood pressure	-0.25	-0.14	-0.33	-0.36	0.06	-0.01
Rate-pressure product	-0.08	-0.14	-0.32	-0.25	-0.24	-0.41*
Cardiac output	-0.43	-0.33	0.22	-0.17	-0.24	-0.30
Peak filling rate	0.17	0.31	0.24	0.54*	0.18	0.26
Initial left ventricular filling rate	-0.23	0.03	0.15	0.23	0.01	0.02
Time-to-peak filling rate	0.46*	0.22	0.08	0.21	0.13	0.26
Myocardial blood flow index	0.19	0.29	-0.28	0.07	0.39	0.40
Myocardial oxidative index	0.37	0.29	-0.24	-0.06	0.30	0.08

Data are the Spearman correlation coefficients. SC, subcutaneous. **P* < 0.05, ***P* < 0.01, ****P* < 0.001.

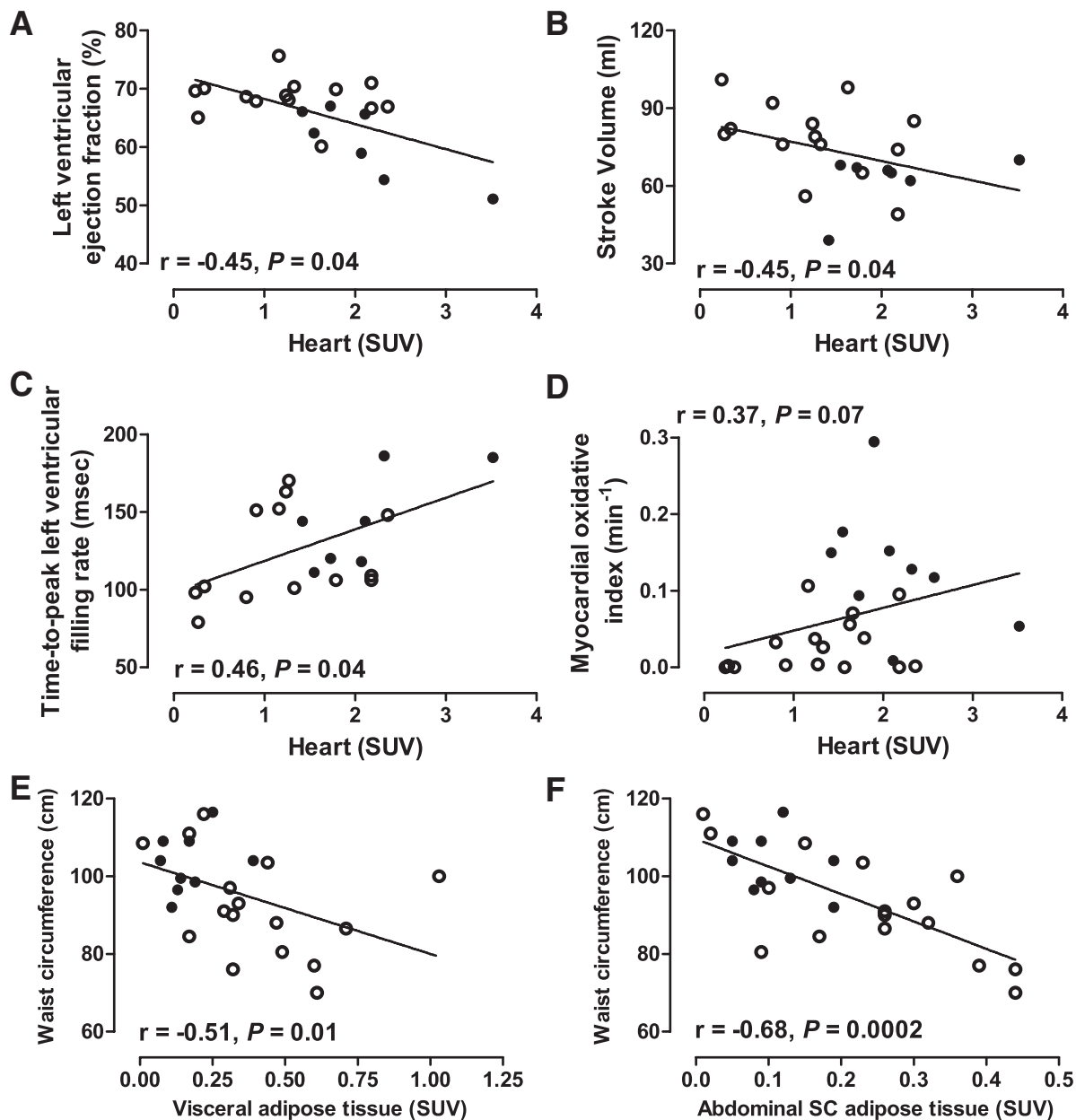


FIG. 5. Spearman correlation between myocardial $14(R,S)$ - ^{18}F THA SUV and left ventricular ejection fraction (A), stroke volume (B), time-to-peak left ventricular filling rate (C), and myocardial oxidative index (D). Spearman correlation between perirenal (visceral) (E) and anterior subcutaneous (SC) abdominal (F) adipose tissues and waist circumference.

Dietary fatty acids contribute to ~25% of VLDL-fatty acids (a marker of hepatic fatty acids) both through chylomicron remnant uptake (~15%) and NEFA spillover from chylomicrons (~10%) (39). Our findings suggest that dietary fatty acids do not significantly contribute to the excess intrahepatic fat accumulation in impaired glucose tolerance. Our method, however, does not distinguish fatty acid oxidation from nonoxidative uptake. We therefore cannot rule out the possibility of reduced hepatic dietary fatty acid oxidation with reciprocal increased deposition in intrahepatic TG. Reduced hepatic γ ATP and inorganic phosphate content are present in T2D and associated with hepatic insulin resistance and increased liver fat content (40).

We also found no significant increase in dietary fatty acid deposition in skeletal muscles of IGT⁺ subjects. We recently showed no increase in leg muscles plasma NEFA uptake

during the postprandial state in subjects with T2D despite increased circulating NEFA levels likely due to reduced muscle blood flow (6). In the current study, we could not measure leg skeletal muscle blood flow as we opted to focus the [^{11}C]acetate kinetic determination in the heart due to the limited PET field of view. ^{18}F THA uptake cannot distinguish between oxidative versus nonoxidative fatty acid metabolism. It is therefore impossible to exclude a reduction in skeletal muscle fatty acid oxidative metabolism with reciprocal increased flux in nonoxidative pathways.

We included all participants that underwent our postprandial PET protocol thus far, resulting in some mismatch for age and sex between the IGT and control groups. We ran post hoc analyses by excluding some controls to match for age or sex as closely as possible and reach the same conclusion as in the main analysis between IGT and controls

(Supplementary Table 2). As IGT participants in our study displayed central obesity and some had hypertension and dyslipidemia, it is also not possible to ascribe the metabolic and cardiac functional abnormalities on IGT per se.

Our new method determines relative organ-specific partition of dietary fatty acids, although determination of absolute uptake rates to organs is more limited. Tissue uptake of dietary fatty acids is very slow, as they appear gradually in circulation because of the delay in gastrointestinal absorption, making this process difficult to model based on dynamic PET acquisitions. We nevertheless could use the Patlak linearization procedure to get some estimates of myocardial and hepatic fractional uptake. Despite the very low and variable blood and tissue signals obtained using list-mode acquisition between 90 and 120 min after meal, myocardial fractional extraction rate showed similar trends to the more robust SUV data obtained using the whole-body scanning approach performed 6 h after oral administration of the tracer. Patlak analysis usually requires taking into account all or most of the area under the curve of blood radioactivity from administration of the tracer up to the time when tissue uptake is assessed. In the case of the current study, blood radioactivity up to time 90 min was not entered into the model. This limitation may affect the absolute fractional uptake value. However, it should be noted that total circulating ^{18}F activity is very low up to time 60 min after oral ingestion of ^{18}F THA (Fig. 2A) (9). Furthermore, plasma ^{18}F activity was similar between the two groups of participants. Thus, this possible bias should not affect group comparison. Although it is not possible to exclude that dietary fatty acid fractional uptake may change over the postprandial period in response, for example, to varying plasma levels of insulin, we found a significant correlation ($r = 0.60$, $P = 0.04$) between cardiac K_i from Patlak analysis performed between time 90 and 120 min after meal and cardiac SUV data that integrate relative uptake over 6 h. Chylomicron-TG activity accounted for less than one-third of plasma ^{18}F activity at time 120 min after meal intake, making our assumptions for the calculation of net myocardial dietary fatty acid uptake dubious. As it is expected for dietary fatty acids, we have shown that orally administered ^{18}F THA readily redistributes into other circulating pools of fatty acids such as NEFA and VLDL-TG from chylomicron-TG in circulation (9). Despite its limitation for the determination of chylomicron-TG-specific fatty acid transport to organs, our method nevertheless simultaneously assesses relative uptake of dietary fatty acids from all circulating sources over most organs. Although ^{18}F THA is trapped into tissues that do not secrete fatty acids such as the heart and skeletal muscles allowing for accurate estimates of dietary fatty acid partitioning in these tissues, our method probably underestimates integrated uptake in tissues such as the liver that can secrete ^{18}F THA as VLDL-TG, or adipose tissues, that may recirculate ^{18}F THA as plasma NEFA. However, dietary fatty acids are recycled in a similar manner.

Our PET ventriculography method was validated in rats and used with success to show differential cardiac function in animals with diabetic cardiomyopathy (10). However, it has never been directly compared with other methods to assess cardiac volumes in humans. Furthermore, to our knowledge, no other group has reported postprandial cardiac function in humans using any method. It is possible that the latter explains why we found reduced left ventricular stroke volume and ejection fraction in IGT

participants in contrast to no changes observed by others (24). Although we are confident about the validity of PET ventriculography to demonstrate relative changes in cardiac function, the absolute cardiac volumes we report may be of limited accuracy.

In conclusion, individuals with IGT and other metabolic features of prediabetes display increased myocardial dietary fatty acid partitioning associated with early impairment in left ventricular systolic and diastolic functions and increased cardiac oxidative metabolism. This suggests a potential role for abnormal dietary fatty acid partitioning and metabolism in the development of metabolic cardiomyopathy in humans. Despite the presence of reduced relative dietary fatty acid uptake in abdominal fat depots that was directly associated with abdominal obesity, we found no increase in hepatic and skeletal muscle dietary fatty acid uptake in IGT. Our findings demonstrate the heterogeneity of mechanisms leading to excess exposure of lean organs to dietary fatty acids in prediabetes.

ACKNOWLEDGMENTS

This work was supported by a grant from the Canadian Institutes of Health Research (MOP 53094 to A.C.C.) and was performed at the Centre de Recherche Clinique Etienne-Le Bel, a research center funded by the Fonds de la Recherche en Santé du Québec. S.M.L. is the recipient of a Canadian Diabetes Association Doctoral Studentship Award. A.C.C. is the recipient of the Canadian Institutes of Health Research–GlaxoSmithKline Chair in Diabetes.

No potential conflicts of interest relevant to this article were reported.

S.M.L., T.G.-L., C.N., S.P., B.G., E.E.T., and A.C.C. were responsible for the collection, analysis, and interpretation of data. S.M.L., B.G., E.E.T., and A.C.C. drafted the manuscript or revised it critically for important intellectual content. A.C.C. was responsible for the conception and design of the experiments. A.C.C. is the guarantor of this work and, as such, had full access to all the data in the study and takes responsibility for the integrity of the data and the accuracy of the data analysis.

REFERENCES

- Giacca A, Xiao C, Oprescu AI, Carpentier AC, Lewis GF. Lipid-induced pancreatic β -cell dysfunction: focus on in vivo studies. *Am J Physiol Endocrinol Metab* 2011;300:E255–E262
- Bickerton AS, Roberts R, Fielding BA, et al. Adipose tissue fatty acid metabolism in insulin-resistant men. *Diabetologia* 2008;51:1466–1474
- Ravikumar B, Carey PE, Snaar JE, et al. Real-time assessment of postprandial fat storage in liver and skeletal muscle in health and type 2 diabetes. *Am J Physiol Endocrinol Metab* 2005;288:E789–E797
- Brassard P, Frisch F, Lavoie F, et al. Impaired plasma nonesterified fatty acid tolerance is an early defect in the natural history of type 2 diabetes. *J Clin Endocrinol Metab* 2008;93:837–844
- Normand-Lauzière F, Frisch F, Labbé SM, et al. Increased postprandial nonesterified fatty acid appearance and oxidation in type 2 diabetes is not fully established in offspring of diabetic subjects. *PLoS ONE* 2010;5:e10956
- Labbé SM, Croteau E, Grenier-Larouche T, et al. Normal postprandial nonesterified fatty acid uptake in muscles despite increased circulating fatty acids in type 2 diabetes. *Diabetes* 2011;60:408–415
- Goldberg IJ, Eckel RH, Abumrad NA. Regulation of fatty acid uptake into tissues: lipoprotein lipase- and CD36-mediated pathways. *J Lipid Res* 2009;50(Suppl.):S86–S90
- Yagyu H, Chen G, Yokoyama M, et al. Lipoprotein lipase (LpL) on the surface of cardiomyocytes increases lipid uptake and produces a cardiomyopathy. *J Clin Invest* 2003;111:419–426
- Labbé SM, Grenier-Larouche T, Croteau E, et al. Organ-specific dietary fatty acid uptake in humans using positron emission tomography coupled to

- computed tomography. *Am J Physiol Endocrinol Metab* 2011;300:E445–E453
10. Ménard SL, Croteau E, Sarrhini O, et al. Abnormal in vivo myocardial energy substrate uptake in diet-induced type 2 diabetic cardiomyopathy in rats. *Am J Physiol Endocrinol Metab* 2010;298:E1049–E1057
 11. Ci X, Frisch F, Lavoie F, et al. The effect of insulin on the intracellular distribution of 14(R,S)-[18F]Fluoro-6-thia-heptadecanoic acid in rats. *Mol Imaging Biol* 2006;8:237–244
 12. Klein LJ, Visser FC, Knaapen P, et al. Carbon-11 acetate as a tracer of myocardial oxygen consumption. *Eur J Nucl Med* 2001;28:651–668
 13. Croteau E, Lavallée E, Labbe SM, et al. Image-derived input function in dynamic human PET/CT: methodology and validation with ¹¹C-acetate and ¹⁸F-fluorothioheptadecanoic acid in muscle and ¹⁸F-fluorodeoxyglucose in brain. *Eur J Nucl Med Mol Imaging* 2010;37:1539–1550
 14. van den Hoff J, Burchert W, Börner AR, et al. [1-(11)C]Acetate as a quantitative perfusion tracer in myocardial PET. *J Nucl Med* 2001;42:1174–1182
 15. Matthews DR, Hosker JP, Rudenski AS, Naylor BA, Treacher DF, Turner RC. Homeostasis model assessment: insulin resistance and beta-cell function from fasting plasma glucose and insulin concentrations in man. *Diabetologia* 1985;28:412–419
 16. Peterson LR, Herrero P, Schechtman KB, et al. Effect of obesity and insulin resistance on myocardial substrate metabolism and efficiency in young women. *Circulation* 2004;109:2191–2196
 17. Jensen MD, Sarr MG, Dumesic DA, Southorn PA, Levine JA. Regional uptake of meal fatty acids in humans. *Am J Physiol Endocrinol Metab* 2003;285:E1282–E1288
 18. McQuaid SE, Hodson L, Neville MJ, et al. Downregulation of adipose tissue fatty acid trafficking in obesity: a driver for ectopic fat deposition? *Diabetes* 2011;60:47–55
 19. Boudina S, Abel ED. Diabetic cardiomyopathy revisited. *Circulation* 2007;115:3213–3223
 20. Diamant M, Lamb HJ, Groeneveld Y, et al. Diastolic dysfunction is associated with altered myocardial metabolism in asymptomatic normotensive patients with well-controlled type 2 diabetes mellitus. *J Am Coll Cardiol* 2003;42:328–335
 21. Whalley GA, Gusso S, Hofman P, et al. Structural and functional cardiac abnormalities in adolescent girls with poorly controlled type 2 diabetes. *Diabetes Care* 2009;32:883–888
 22. Ng AC, Delgado V, Bertini M, et al. Myocardial steatosis and biventricular strain and strain rate imaging in patients with type 2 diabetes mellitus. *Circulation* 2010;122:2538–2544
 23. Zhou YT, Grayburn P, Karim A, et al. Lipotoxic heart disease in obese rats: implications for human obesity. *Proc Natl Acad Sci USA* 2000;97:1784–1789
 24. McGavock JM, Lingvay I, Zib I, et al. Cardiac steatosis in diabetes mellitus: a ¹H-magnetic resonance spectroscopy study. *Circulation* 2007;116:1170–1175
 25. Szczepaniak LS, Victor RG, Orci L, Unger RH. Forgotten but not gone: the rediscovery of fatty heart, the most common unrecognized disease in America. *Circ Res* 2007;101:759–767
 26. Reingold JS, McGavock JM, Kaka S, Tillery T, Victor RG, Szczepaniak LS. Determination of triglyceride in the human myocardium by magnetic resonance spectroscopy: reproducibility and sensitivity of the method. *Am J Physiol Endocrinol Metab* 2005;289:E935–E939
 27. Taha M, Lopaschuk GD. Alterations in energy metabolism in cardiomyopathies. *Ann Med* 2007;39:594–607
 28. Ouwens DM, Diamant M, Fodor M, et al. Cardiac contractile dysfunction in insulin-resistant rats fed a high-fat diet is associated with elevated CD36-mediated fatty acid uptake and esterification. *Diabetologia* 2007;50:1938–1948
 29. Chess DJ, Stanley WC. Role of diet and fuel overabundance in the development and progression of heart failure. *Cardiovasc Res* 2008;79:269–278
 30. Ménard SL, Ci X, Frisch F, et al. Mechanism of reduced myocardial glucose utilization during acute hypertriglyceridemia in rats. *Mol Imaging Biol* 2009;11:6–14
 31. Wright JJ, Kim J, Buchanan J, et al. Mechanisms for increased myocardial fatty acid utilization following short-term high-fat feeding. *Cardiovasc Res* 2009;82:351–360
 32. Romanski SA, Nelson RM, Jensen MD. Meal fatty acid uptake in adipose tissue: gender effects in nonobese humans. *Am J Physiol Endocrinol Metab* 2000;279:E455–E462
 33. Uranga AP, Levine J, Jensen M. Isotope tracer measures of meal fatty acid metabolism: reproducibility and effects of the menstrual cycle. *Am J Physiol Endocrinol Metab* 2005;288:E547–E555
 34. Votruba SB, Jensen MD. Sex-specific differences in leg fat uptake are revealed with a high-fat meal. *Am J Physiol Endocrinol Metab* 2006;291:E1115–E1123
 35. McQuaid SE, Humphreys SM, Hodson L, Fielding BA, Karpe F, Frayn KN. Femoral adipose tissue may accumulate the fat that has been recycled as VLDL and nonesterified fatty acids. *Diabetes* 2010;59:2465–2473
 36. Santosa S, Hensrud DD, Votruba SB, Jensen MD. The influence of sex and obesity phenotype on meal fatty acid metabolism before and after weight loss. *Am J Clin Nutr* 2008;88:1134–1141
 37. Mårin P, Lönn L, Andersson B, et al. Assimilation of triglycerides in subcutaneous and intraabdominal adipose tissues in vivo in men: effects of testosterone. *J Clin Endocrinol Metab* 1996;81:1018–1022
 38. Votruba SB, Mattison RS, Dumesic DA, Koutsari C, Jensen MD. Meal fatty acid uptake in visceral fat in women. *Diabetes* 2007;56:2589–2597
 39. Barrows BR, Parks EJ. Contributions of different fatty acid sources to very low-density lipoprotein-triacylglycerol in the fasted and fed states. *J Clin Endocrinol Metab* 2006;91:1446–1452
 40. Szendroedi J, Chmelik M, Schmid AI, et al. Abnormal hepatic energy homeostasis in type 2 diabetes. *Hepatology* 2009;50:1079–1086